Solar Energy 162 (2018) 525–532

Contents lists available at ScienceDirect

Solar Energy

journal homepage: www.elsevier.com/locate/solener

Tuneable and spectrally selective broadband reflector – Modulated photonic crystals and its application in solar cells

Anishkumar Soman, Aldrin Antony*

Department of Energy Science and Engineering, Indian Institute of Technology Bombay, Mumbai 400076, India

ARTICLE INFO

Keywords:
Photonic crystal
Broad band reflector
Light trapping
Back reflector
Solar cell

ABSTRACT

One dimensional photonic crystal has been developed as a broadband dielectric reflector, the stopband of which could be selectively tuned based on absorption spectrum of the absorber material. The design parameters and factors which contribute to the tunability of the photonic crystals are analyzed through simulations and experiments. The photonic crystal structures are fabricated using silicon rich silicon nitride and silicon oxynitride thin films deposited by PECVD at 200 °C. Modulated photonic crystal with a broad bandwidth, having an integrated reflectance of 97.6% in the wavelength range 580–1200 nm has been fabricated and applied in an amorphous silicon thin film solar cell as the back reflector. The optical performance of solar cells with these back reflectors has been studied in the longer wavelength as against the conventional metallic back reflector. The characterization of the thin film silicon solar cell with these photonic structures presented a short circuit current density of 14.77 mA/cm^2. The angle dependent behaviour of the photonic crystal has been studied using angle dependent current-voltage measurement and a future prospectus of these structures as passivation layer for ultra thin crystalline silicon solar cells is also highlighted.

1. Introduction

With the prospect of reducing the cost of electricity from solar energy, it is imperative to decrease the overall cost of solar cell by reduced material usage. Therefore the decrease in thickness of the solar cell has to be accompanied by light trapping methodologies for improved efficiency of the solar cell. One of the conventional ways to achieve enhanced light trapping is by having a nearly 100% Lambertian back reflector which will diffusely reflect light back into the active thin film solar material. The back reflector coupled with scattering at the textured surface will increase the optical path travelled by light through multiple reflections in the cell and hence increase in light absorption. Therefore if we have a dielectric slab having a perfect 100% Lambertian scattering at the back coupled with front texture then the hypothetical classical absorption limit (Yablonovitch, 1982; Tiedje et al., 1984) is given by $4n^2$ where n is the real part of the complex refractive index of the dielectric slab. In case of a solar cell where the dielectric slab is silicon wafer having a refractive index n = 3.5 then light trapping can theoretically improve the absorption factor by 50 (Yablonovitch and Cody, 1982). The light trapping plays a crucial role in achieving higher efficiencies for the different thin film and ultra-thin c-Si solar cells. In the case of thin film silicon solar cells, the conventional metallic back reflector like silver (Ag) have high reflectance however the textured surface of the metal suffer from surface plasmon absorption losses (Springer et al., 2004). An alternate back reflector can be a Bragg reflector also called as one dimensional photonic crystal (Yablonovitch, 1987) (1DPC), which could ideally reflect near to 100% light over a specific wavelength band. 1DPC are structures in which there is periodic arrangement of varying dielectric media along a single axis (along one dimension) in such a way that the periodicity results in a periodic dielectric function for the propagating light wave. The periodic stack has alternate high and low refractive index material; and light gets scattered from each interface. If the optical path length between two light waves from the interface is half of the wavelength of light then they interfere constructively such that there is no net transfer of energy in the forward direction. The range of frequencies for which the photon is forbidden in the forward direction is called a Photonic stopband and the structure so fabricated is called a quarter wave stack photonic crystal. Though extensive work has been done on integrating photonic crystals with plasmonic grating for enhanced light harvesting (Biswas and Xu, 2012; Zeng et al., 2008; Zhou and Biswas, 2008) by creating resonant modes of surface plasmon-polaritons which will confine light waves to the interface, these methodologies require additional lithography and etching steps which further increase the complexity of cell processing. 1DPC are relatively simpler to fabricate and uses the same deposition technique which is currently used in commercial solar cells

* Corresponding author.
E-mail address: aldrinantony@iitb.ac.in (A. Antony).

https://doi.org/10.1016/j.solener.2018.01.061
Received 24 September 2017; Received in revised form 5 December 2017; Accepted 18 January 2018

and hence can be easily integrated to cell fabrication pilot line. In this paper we have developed a Photonic crystal for which the photonic stopband can be selected and tuned as per the spectral requirement of the solar cell in addition to the "modulated" features (Krc et al., 2009), hence referred as Tuneable and Spectrally Selective Broadband Reflector Modulated Photonic Crystal (TSSBR-MPC).

TSSBR-PC is fabricated using alternate layers of high and low refractive index materials in such a way that the Photonic Band Gap (PBG – range of frequencies over which light gets reflected completely from the PC) (Yablonovitch, 1987; O'Brien et al., 2008) can be selected as per the absorption spectrum of the solar cell by changing the thickness, number of layers and by using varying refractive index materials (Krc et al., 2009). This selectivity in reflection can be extremely beneficial for different types of Solar cells as the reflector can be custom made for the specific cell. There are also reports on the application possibility of PC back reflectors for monocrystalline (Zeng et al., 2006) and multicrystalline (Ivanov et al., 2009) solar cells to improve the light trapping. Different types of Bragg reflectors have been proposed as the back reflector for thin film solar cells and a few groups have reported their integration in amorphous and microcrystalline thin film silicon solar cells (Krc et al., 2009; Mutitu et al., 2010; Kuo et al., 2012; Isabella et al., 2012), dye sensitized solar cells (Colodrero et al., 2012; Heiniger et al., 2013), organic and polymer solar cells (Lunt and Bulovic, 2011; Yu et al., 2013; Betancur et al., 2013), III-V solar cells (Johnson et al., 2005; Tsai et al., 2013; Tobin et al., 1991) and thermophotovoltaics (Florescu et al., 2007). One of the interesting applications of TSSBR-PC would be in "micromorph" tandem cells (Fischer et al., 1996) and triple junction solar cells (Yan et al., 2006; Kim et al., 2013) where a modified TSSBR-PC can act as selective intermediate reflector for a-Si:H, a-SiGe:H and μc-Si:H having bandgap 1.75, 1.45 and 1.1 eV respectively. In this application as selectively reflecting intermediate reflector, for each absorber layer it would reflect only the desired spectral range of light which can be absorbed by that absorber layer, whereas it will act as an intermediate window for the remaining wavelength of light. In this paper we are presenting the design principles underlying the fabrication of TSSBR-MPC through simulation and experiment and the characterization of the TSSBR-MPC that we fabricated. As a proof of concept we have integrated TSSBR-PC in thin film amorphous silicon solar cells and the performance for the cells with different reflectors at the bottom are compared. The application potential of dielectric reflectors as the back surface passivation layer and reflectors for ultrathin crystalline silicon solar cells is also presented.

Along with the multitudinous applications mentioned above, it is also important to emphasize on the plausible applications of TSSBR-PC in silicon wafer photovoltaic technology. P-type c-Si solar cells with Al-BSF suffer from high recombination losses at the rear side and parasitic absorption losses (Ingenito et al., 2014a). The longer minority carrier life times, less sensitivity to impurities of n-type wafers, absence of boron-oxygen complexes as observed in p-type wafers, no light induced degradation, potential to give high open circuit voltage and high conversion efficiency has generated considerable interest for n-type silicon solar cells recently (Ingenito et al., 2016). Bifacial solar cells with high conversion efficiencies have been demonstrated (Böscke et al., 2013) and industries have shown interest in these bifacial modules since there is no additional cost in cell and module manufacturing processes, could be easily implemented in the current production lines and are scalable for commercial production. The bifacial cell with light coming from both sides is not practical at all geographical locations, since the albedo light may be insufficient. In such cases, a white reflector film is preferred to be used at the rear side, but is limited with their reflectivity around 85% (Alcántara et al., 2014). Metal free reflectors based on distributed bragg reflectors which could have nearly 100% reflectivity has been proposed as a replacement for white reflecting films to enhance the light trapping by Ingenito et al. (2016). Another interesting possibility of these dielectric mirrors is their dual nature which we have demonstrated earlier (Soman and Antony, 2017); where they will act as nearly 100% reflectors and by suitably selecting the first dielectric material in the stack, they would also act as a passivating stack for achieving higher life time. By carefully choosing Silicon Oxynitride (SiON) or non-stoichiometric Silicon Nitride (SiN) as the first layer of the dielectric stack we could passivate p or n-type surfaces effectively.

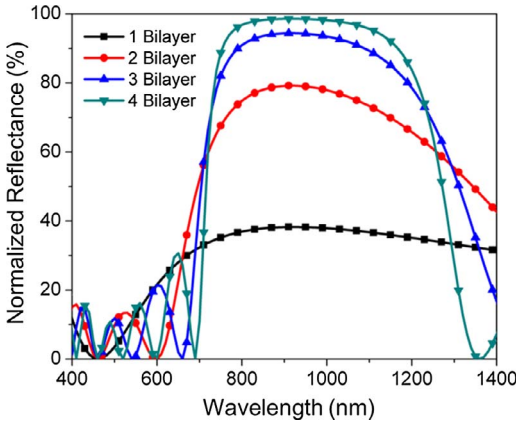

Fig. 1. The simulated reflectivity curves of photonic crystals with different number of bilayers.

Another area of application of our work is in ultra-thin crystalline silicon solar cells since light trapping is a vital aspect in thin silicon substrates due to the low absorption coefficient in the near infrared region of the solar spectrum and can help to achieve low cost flexible solar cells without sacrificing efficiency (del Cañizo et al., 2009; Goodrich et al., 2013). Ultrathin silicon solar cells are an area of interest since they further reduce production cost, use lesser raw material, reduce bulk recombination and light induced degradation (Ingenito et al., 2014b). Ingenito et al. (2014b) has already demonstrated light trapping structures showing absorption very close to $4n^2$ classical limit in ultrathin c-Si solar cells using distributed back reflector at the rear side along with random pyramidal structure. With wafers less than 35 μm achieving 99.8% implied photocurrent density it is possible to fabricate ultrathin c-Si solar cells with these advance light trapping schemes.

2. Experimental details

The fabrication of the Photonic Crystal (PC) has been done using a parallel plate radio frequency plasma-enhanced chemical vapor deposition (rf-PECVD) system. We have used alternating layers of hydrogenated amorphous Silicon Nitride (a-Si_xN_y:H) and Silicon Oxynitride (a-SiO_xN_y:H) thin films having different compositions (Soman and Antony, 2017) for making tunable and selective reflector. The a-Si_xN_y:H films mentioned in this paper are deviated from their stoichiometry and are made silicon rich, hence it will be mentioned as Silicon Rich Silicon Nitride (SRSN) in the remaining part of the text unless and otherwise specified. SRSN layers were deposited by varying ammonia (NH_3) to silane (SiH_4) gas flow ratio from 1 to 0.0625, and we have obtained SRSN layers of varying refractive index from 2.35 to 3.29 (at 632.8 nm, measured using F40 Filmetrics Reflectometer). Similarly Silicon Oxynitride layers (represented as SiON) with refractive index varying from standard Silicon nitride of 1.95–1.53 were obtained by varying the silane (SiH_4), hydrogen (H_2) and nitrous oxide (N_2O) gas flow ratios. The gas flow ratio for the deposition of SRSN (Q_H) and SiON (Q_L) are given by,

$$Q_H = \frac{\varnothing_{NH_3}}{\varnothing_{SiH_4}} \quad (1)$$

$$Q_L = \frac{\varnothing_{N_2O}}{\varnothing_{N_2O} + \varnothing_{SiH_4}} \quad (2)$$

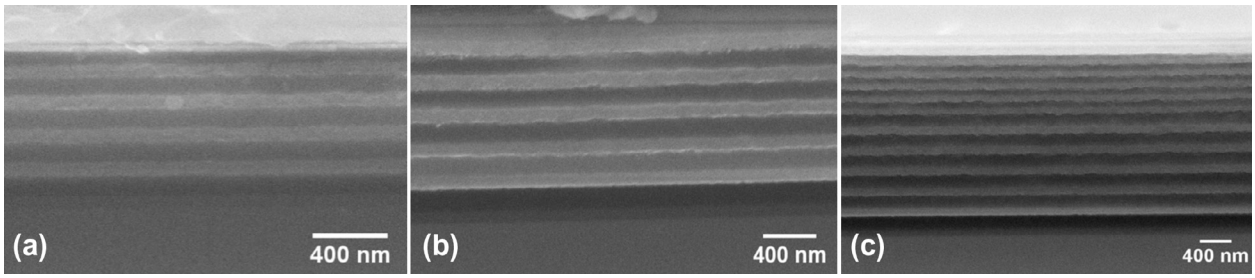

Fig. 2. Cross sectional FESEM of (a) PC 1(SRSN – 45 nm/SiON – 90 nm) (b) PC 2(SRSN – 75 nm/SiON – 150 nm) (c) modulated PC – combination of PC 1 and PC 2 having a total of 12 bilayers.

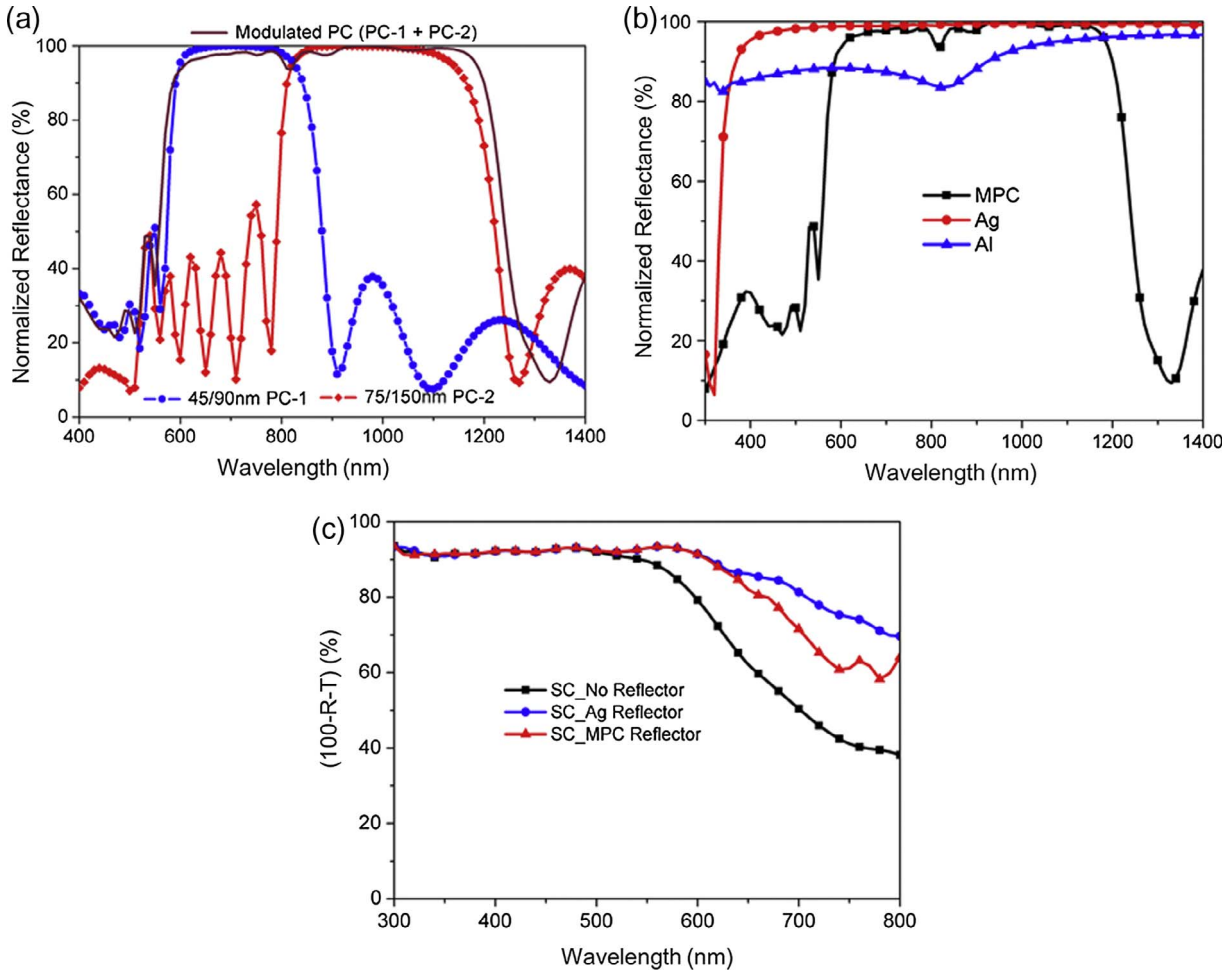

Fig. 3. (a) The measured reflectance of PC 1 and PC 2 along with that of the modulated PC (b) comparison of reflectivity of aluminium (Al), silver (Ag) and modulated photonic crystal (MPC) (c) (100-R-T) graph of a-Si solar cells with different back reflectors.

where, $\varnothing_{NH_3}$, $\varnothing_{SiH_4}$ and $\varnothing_{N_2O}$ are the gas flows of NH_3, SiH_4 and N_2O respectively in sccm. The different films that obtained are named as SRSN_Q_H and SiON_Q_L henceforth. For SiON the flow of H_2 is maintained constant at 20 sccm. All the layers were deposited at a low substrate temperature of 200 °C and at a power density of 60 mW/cm^2 in order to decrease the thermal budget of the process and to be able to be processed inline with the solar cell fabrication without damaging the layers. The distance between the electrode and the substrate is 2.5 cm and the chamber pressure used for deposition is 700 mTorr. SRSN was used as the high refractive index material and SiON as the low refractive material. We have fabricated quarter wavelength stacks of the photonic crystal and the optimization of the thickness and number of layers of the photonic crystal is given elsewhere (Soman and Antony, 2014). The bragg reflector can be designed to have a reflectivity of 1 independent of the angle of incidence and polarization of light by using the equation of omnidirectionality (Chigrin et al., 1999) given by:

$$n_o' = \frac{n_h n_l}{\sqrt{n_h^2 + n_l^2}} > n_o \tag{3}$$

where n_h and n_l are the high and low refractive index of the bragg reflector respectively, n_o is the refractive index of the incident medium. Though the photonic crystal reported in this work hasn't been designed for omnidirectionality the wide stopband of the photonic crystal helps it to have considerable reflection with increase in angle of incidence.

The amorphous silicon solar cell is deposited over commercially available textured Fluorine doped Tin Oxide (SnO_2:F) glass substrates. The a-Si cell was deposited in p-i-n configuration with a 200 nm intrinsic layer by PECVD. Boron doped Zinc Oxide (ZnO:B) of ~1 μm is

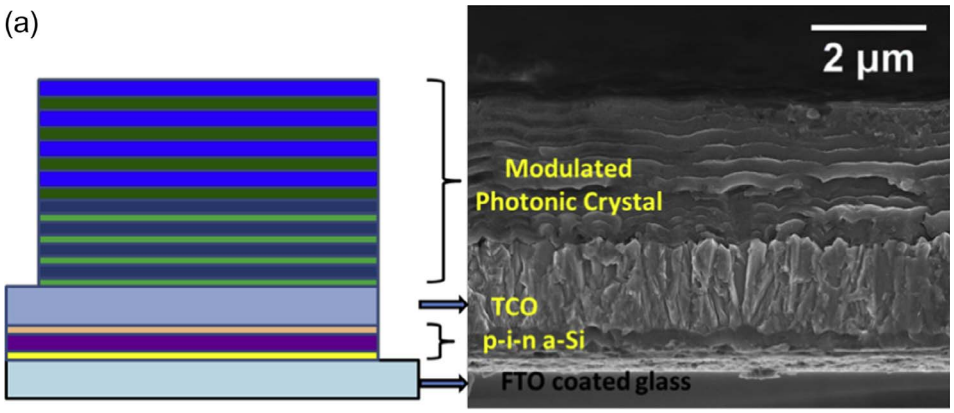

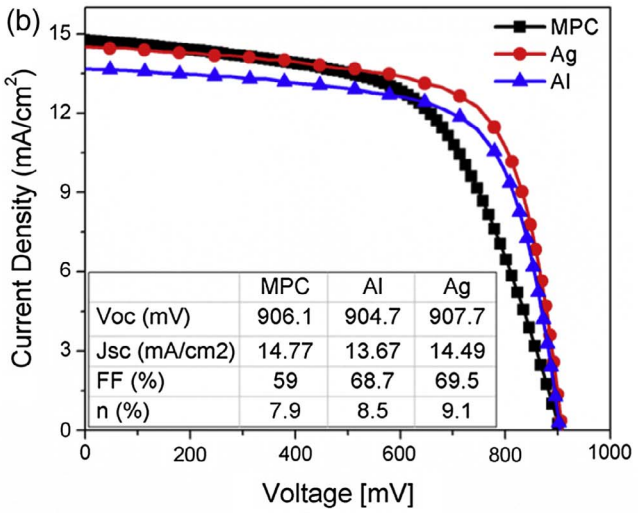

Fig. 4. (a) Schematic structure of a-Si solar cell with TSSBR MPC along with the cross sectional FESEM image of the fabricated solar cell. (b) Current density against voltage characteristic of a-Si solar cell with Ag, Al and MPC backreflector.

deposited over this p-i-n structure which acts as a back contact for the solar cell and helps in carrier collection. TSSBR-MPC deposited over ZnO acts as the back reflector.

In order to study the optical properties of the PC, we have deposited them on Corning 1737F glass and p-type ⟨1 0 0⟩ oriented 4-7Ω-cm resistivity CZ-Si wafer. The transmittance and reflectance measurements were recorded using Perkin Elmer UV–VIS-NIR Spectrometer - Lambda 950 equipped with an integrating sphere. The images of the TSSBR-MPC are taken using Zeiss Ultra 55 Field Emission Scanning Electron Microscopy (FE-SEM). Solar Cell I-V Measurement System by ABET was used to find the I_{sc}, V_{oc}, Fill Factor (FF) and efficiency (η) of the solar cell. The lifetime measurements are done using WCT 120 Photo-conductance Lifetime tester by Sinton Instruments.

The simulations were done using open source RefDex software (Manley et al., 2014) which uses Transfer matrix method to simulate the reflectivity of the photonic crystals. For computing the Reflectivity we consider that the films are non-absorptive, homogeneous, isotropic, non-magnetic and have negligible surface roughness. For comparing the reflected data of the samples from the Spectrophotometer with integrating sphere to the simulated results we have used an incident angle of 8° and the incident light to be unpolarized. We have used simulation to study the effect of factors like number of bilayers, change in refractive indices of the bilayers, angle dependence of photonic crystal and change in thickness of individual layer on the stopband of the photonic crystals. These observations have been correlated with experimental results and the same has been verified in this paper.

3. Results and discussion

The methodology followed for fabricating a TSSBR-PC based on the absorption spectra of different solar cells consist of 2 steps mainly developing a library of materials having varying refractive index and designing a TSSBR-PC by controlling factors like number of layers, refractive index of material and thickness of bilayers to obtain the required photonic stopband. The optimized films used for the fabrication are SRSN with refractive index varying from 3.29 to 2.35 and SiON films with refractive index which lies between 1.95 of stoichiometric Si_3N_4 to 1.53. In order to tune the stopband of the Photonic Crystal we have considered 3 parameters, namely, (i) the number of bilayers, (ii) changing the ratio of refractive indices of the bilayers and, (iii) changing the thickness of the layers.

The ratio of the refractive indices of the materials of the bilayer determines the width of the stopband of the PC. Higher ratio results in widening of the stopband, whereas an increase in the thickness of the bilayers results in a red shift in the stopband spectra of the PC. To understand the effect of number of bilayers we have constructed PC with SRSN_0.125 (n = 3.08) and SiON_0.9 (n = 1.53) as the high & low refractive index materials. The simulation results of the reflectivity of PCs with number of bilayers gradually increasing from 1 to 4 are given in Fig. 1. It shows that with the increase in number of bilayers, the reflectance increases, the band edges become sharpened and the reflectance saturates at nearly 100% after a certain number of bilayers as expected (Xifré Pérez, 2007).

We have found empirically that 6 bilayers is the ideal one with well-defined band edges and nearly 100% reflectance. In addition to these parameters, the bandwidth of the back reflector can be further increased by “Modulating” concepts, wherein multiple photonic crystals having different stopbands are added together to get a single photonic crystal of combined stopbands. In order to fabricate a Modulated PC we have developed 2 PCs having different stopbands by altering their

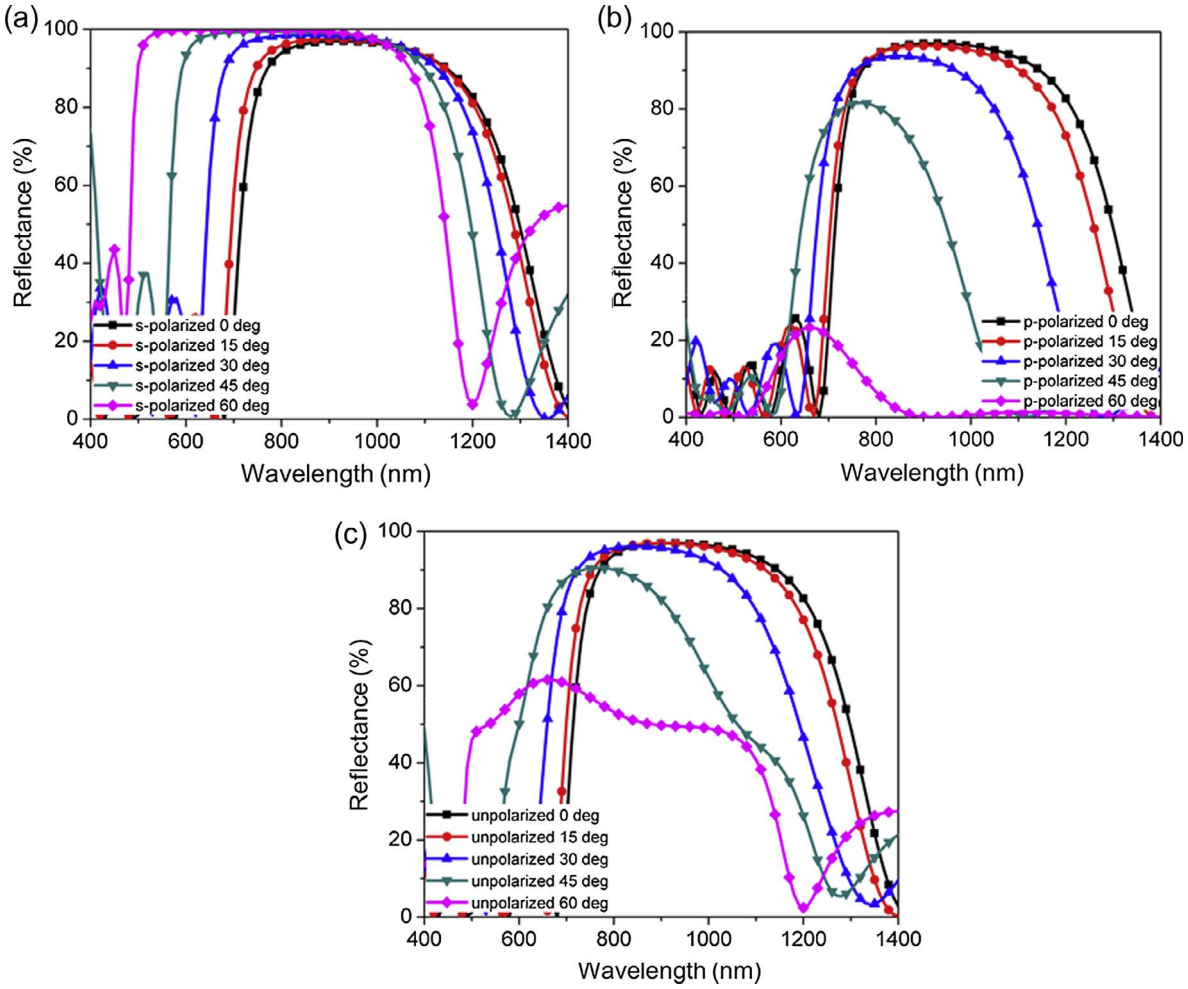

Fig. 5. The simulated reflectance spectra of PC showing the angle dependant variation of the stopband of PC for (a) s-polarized (b) p-polarized and (c) unpolarized light.

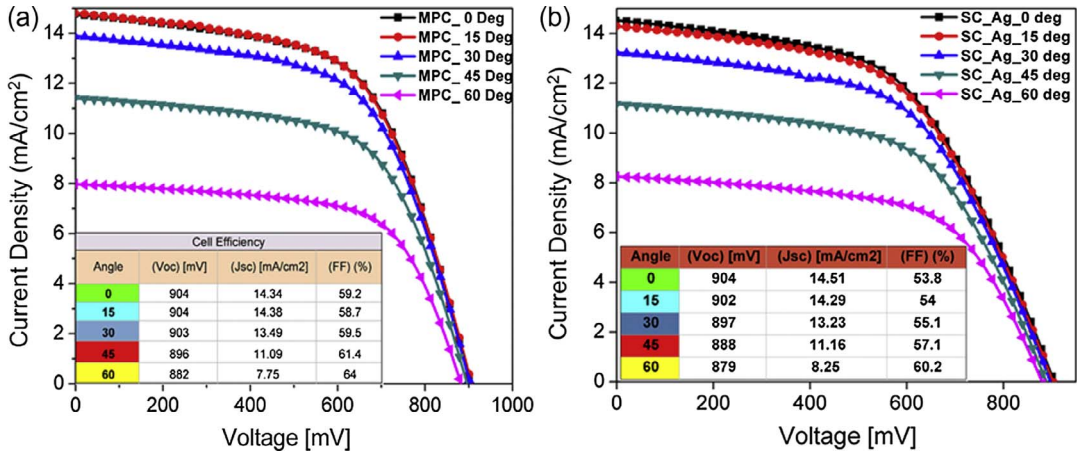

Fig. 6. Angle dependent I-V measurement of a-Si solar cells with (a) MPC backreflector, and (b) Ag back reflector.

thickness. The 1st PC (PC 1) has 6 bilayers each having a thickness of 45 nm SRSN and 90 nm SiON and the 2nd PC (PC 2) also has 6 bilayers having thickness of 75 nm SRSN and 150 nm SiON. Both the PCs are made from the same SRSN_0.125 and SiON_0.9. The Modulated PC has a total of 12 bilayers which is the combination of PC 1 and PC 2 and the cross sectional FESEM image of these structures are given in Fig. 2. The reflectance of the individual PCs and that of the modulated PCs are shown in Fig. 3a. PC 1 has a stopband from 585 to 850 nm, whereas PC 2 has a stopband from 805 to 1200 nm. The reflectivity of the MPC has a combined stopband of PC 1 and PC 2 having a bandwidth of 620 nm from 580 to 1200 nm with an integrated reflectance of 97.6%.

After showing the feasibility of fabricating broad band reflecting MPC, we investigated the reflectivity of the dielectric MPC in comparison with metallic reflectors like Al and Ag which are typically used as the back contact as well as reflector. Fig. 3b shows the reflection spectra of Ag, Al and MPC; it can be observed that Al has an integrated reflection of 87.6% in the visible range (400–700 nm) however it has a dip in the reflectivity in the near infrared region. Ag has high integrated

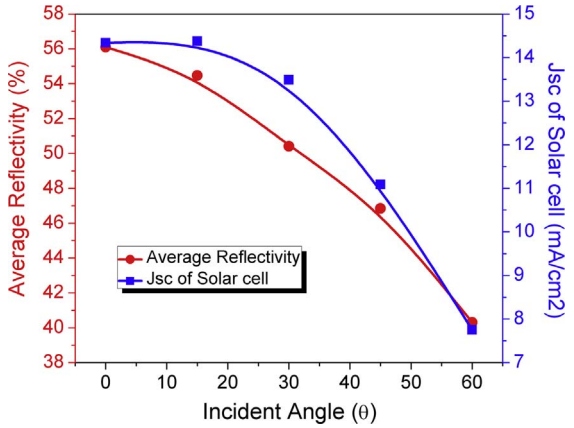

Fig. 7. The simulated average reflectivity of the PC in the wavelength range 300–1400 nm and the measured short circuit current density (J_{sc}) of a-Si solar cells with MPC back reflector at different angle of incidences.

Table 1
Measured and percent decrease in J_{sc} values at different angle of incidence for a-Si cells with MPC and Ag back reflector.

Incident angle (°)	Solar cells with MPC		Solar cells with Ag	
	Measured J_{sc} [mA/cm^2]	% decrease in J_{sc} with the normal incidence	Measured J_{sc} [mA/cm^2]	% decrease in J_{sc} with the normal incidence
0	14.34	–	14.51	–
15	14.38	−0.3	14.29	1.5
30	13.49	5.9	13.23	8.8
45	11.09	22.7	11.16	23.1
60	7.75	46.0	8.25	43.2

reflectance of 98.9% over a broad spectrum from visible to near infrared (400–1200 nm) and an integrated reflectance of 98.2% in the visible range of the spectrum. However it is economically expensive to use Ag as back reflector. As against plain Ag surface, textured Ag surface suffers from surface plasmon polariton (SPP) losses at the metal dielectric interface and may critically influence the performance while applied in thin film solar cells. Also the SPP effect becomes prominent when the Ag surface has arbitrary texture. The SPP excitation not only results in absorption losses but also reduces scattering of light by metal back contact (Haug et al., 2008). Therefore the advantage of this TSSBR MPC gets highlighted in solar cell application where the metal back contact is textured and the losses due to SPP can become evident. As against this metal contact on textured substrate surfaces, the TSSBR MPC is a dielectric stack which gives the reflectivity comparable to Ag metal in the desired wavelength range of the solar cell and wouldn't show plasmonic absorption losses. In this case we can see that from 580 to 1200 nm the MPC gives higher reflectivity than Al and gives ~100% reflectivity like Ag in the stopband regime of the MPC. The MPC has an integrated reflectance of 97.3% in the weak absorption regime of 600–800 nm in a-Si cells, and an integrated reflectance of 98% for 600–1100 nm as against 99.3% and 89.1% for Ag and Al respectively in the same bandwidth. Thus we aim to fabricate solar cells having comparable results with Ag back reflector which we consider as a nearly ideal reflector.

In order to show the effectiveness of the as demonstrated dielectric reflector, we have coated the a-Si cells with metallic Ag reflector as well as dielectric MPC reflector and performed the optical analysis. The integrated transmittance of the solar cell from 500 nm to 800 nm is 25% for cell with no reflector and this can be reduced to 3.6% for cell with MPC back reflector which amounts to ~85% decrease in transmission losses. In order to gain knowledge in the longer wavelength region where the light trapping improvement is needed, (100-R-T) graph of the a-Si cells is presented in Fig. 3c which shows the increase in absorption of light by the active material of the a-Si cells from 600 to 800 nm which otherwise isn't harvested for carrier generation in the cell. By analyzing the data from Fig. 3c, we get that the integrated absorbance of the cell between 500 and 800 nm increases from 64.7% for cell without any reflector to 79.3% for cell with MPC back reflector and 84.5% absorbance for Ag back reflector cell in the same wavelength range. This account for a 22.6% increase in absorption in the above wavelength range for a solar cell with MPC back reflector as compared to cell with no back reflector; whereas cell with Ag back reflector increase the absorbance by 30.6%.

The schematic cell structure of the a-Si cell with the TSSBR MPC along with its cross sectional FESEM is shown in Fig. 4a. The different layers of the solar cells could be clearly identified from the SEM image. The IV measurement depicts that the cell with MPC back reflector has comparable results with the cell with Ag back reflector and the same is shown in Fig. 4b. The lighted I-V measurement of the solar cells was done and the cell with the MPC back reflector presented a current density of 14.77 mA/cm^2 which is much closer to the J_{sc} of Ag back reflector cell of 14.49 mA/cm^2. The decrease in fill factor for MPC cells is due to the non-optimized contacting method to the back TCO, parasitic losses caused by smaller contact area of TCO with the metal contact pad resulting in a comparatively lesser efficiency.

The stopband of the photonic crystal is expected to be angle dependent and hence in order to understand the effect of the angle dependence on the reflectance, we simulated the effect using 4 bilayer PC on glass substrate by varying the incident angle of light from 0° to 60° in

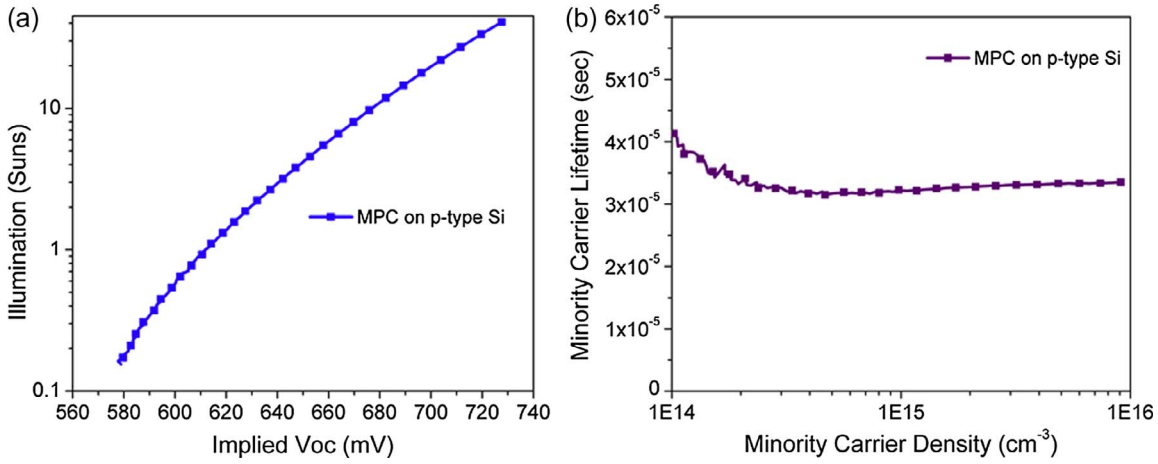

Fig. 8. (a) Implied V_{oc} versus illumination and, (b) lifetime versus minority carrier density for p-type CZ wafers with MPC on one side.

steps of 15°. As can be seen in Fig. 5 for s-polarized light when the incident angle increases, the stopband has a blue shift and the reflectivity increases. On the other hand for p-polarized light the reflectivity drastically decreases from stopband peak of 96% reflectivity at 0° to 23% peak reflectivity at 60° along with the shift of the stopband to the lower wavelength. This is attributed to the interaction of the transverse electric field (p-polarized) part of the light wave with the electric dipoles at the interface. Therefore the effective stopband of the PC is the cumulative effect of the s and p polarized light and the same can be observed in the reflectivity for unpolarized light. The stopband of the PC shows a shift to the lower wavelength as the incident angle increases as expected and also the reflectivity decreases. The shift of the stopband can be overcome by designing a TSSBR MPC having a stopband considerably wider than the band edge of the material. Therefore the TSSBR MPC designed for a-Si cells having band edge at 780 nm has a stopband till 1200 nm to compensate for the band shift at varying angles.

To understand a real time working of the solar cell with MPC back reflector at different angles we performed a varying angle I-V measurement by using a rotatable chuck for the same angle variation of 0°–60° with a step of 15° as shown in Fig. 6a. We have used a different set of samples for doing the I-V measurement mentioned in Fig. 4 and angle dependent I-V in Fig. 6 since the silver contacts of the samples degrade with time on exposure to ambient humid conditions. The cell efficiency and the J_{sc} of the cell remains almost consistent at 0° and 15°; the same trend is observed for the simulated stopband of the PC which tends to overlap for these small angles. The J_{sc} drops drastically from 13.49 mA/cm^2 to 7.75 mA/cm^2 for cells with MPC back reflector when the incident angle changes from 30° to 60°. Though the J_{sc} varies with the angle of incidence it might not be a direct indication of the angle dependence of the photonic crystal and could be related to the change in front side reflection with angle of incidence. We tried to correlate the average reflectivity of the simulated PC over 300–1400 nm to the Jsc values at different angle of incidence and found a similar trend as shown in Fig. 7. In order to verify if the decline in J_{sc} is due to the angle dependence of the PC we performed an angle dependent I-V measurement for cells with Ag back reflector. We found that for the cells with Ag back reflector also had a declining J_{sc} value trend as depicted in the graph of Fig. 6b. Therefore we associate the decreasing J_{sc} to change with effective cell area while doing the angle dependent I-V measurement since the reflectivity of Ag is independent of angle of incidence. As the angle changes the effective area for the photon flux is ACosθ where A is the active cell area. In Table 1 we have compared the percent decrease in J_{SC} at various angles for solar cells with MPC and Ag back reflector. We observe that the difference in % of decrease in J_{sc} between MPC and Ag back reflector solar cells is within 2–3% across the entire range of angles from 0° to 60°. Thus we can consider that the loss due to the angle dependent stopband of the PC has negligible effect on the actual performance of the solar cells.

The versatility of TSSBR-MPC structure could also find application in c-Si solar cells. It is interesting to note that for a c-Si cell MPC structure can not only contribute to improve the J_{sc} but also improve V_{oc} of the cell by improving the passivation of the back surface if it is carefully engineered. The SiON of the PC which acts as the 1st layer to be in contact with the p-type c-Si cells tend to passivate the interface as these layers are hydrogenated. We have seen that CZ wafer having a base lifetime of 6 μs (without any coating) improved to 32.1 μs at a minority carrier density (MCD) of 10^{15} cm^{-3} with the help of PC coated at one of its surface. This demonstrates that the PC helps to increase the lifetime up to ~5 times and the lifetime versus MCD results are shown in Fig. 8a. It can also been seen from Fig. 8b that the PC on p-type cells give an implied V_{oc} of 612 mV at 1 sun illumination. It should also be noted that here only a single side passivation of the c-Si wafer is performed. These values can be further increased by improving the passivating quality of the SiON which we intend to include in our future work. The metallization for such a thick layer of photonic crystal backreflector can be done by the conventional screen-printing of the metal paste followed by the firing as has been demonstrated by Ingenito et al. (2014b) and a cost effective method can be opening the dielectric using laser (Xu et al., 2017) and metal contacts can be made by Ni−Cu plating (Raval et al., 2015) to incorporate the dielectric mirrors to c-Si solar cells. The importance of such light trapping structures will become predominant in thinner c-Si cells where the long wavelength photons will not be effectively absorbed as the absorption length will be more than the actual thickness of the cell.

4. Conclusion

TSSBR MPC offers a great prospectus for light trapping for different solar cells which requires light management techniques. In this paper we have fabricated a TSSBR MPC having an integrated reflectance of 97.6% over a broad wavelength range of 580–1200 nm. To prove the proof of concept we have shown that MPC back reflector reduces the transmission losses to 3.6% in a-Si solar cells and the absorbance of the cell is 79.3% with MPC back reflector in the wavelength range of 500–800 nm which is comparable to 84.5% absorbance of cells with Ag back reflector. On applying the MPC back reflector to device we get a J_{sc} of 14.77 mA/cm^2 as compared to cell with Ag back reflector having J_{sc} value of 14.49 mA/cm^2. These structures can not only replace the conventional metallic back reflectors which suffer from surface plasmon absorption losses but can also be tuned based on the bandgap on any absorber material thereby can find application in any type of solar cell technology which requires light trapping. If properly engineered, it can even act as a selective intermediate reflector in tandem cells which reflects back the shorter wavelength to top cell and transmit the longer ones to bottom cell. As technology advances ultrathin silicon solar cells will find necessity for such back reflectors thereby overcoming the losses due to low absorption coefficient of silicon for longer wavelength photons. Back reflector will play a crucial role in such cells in which the back surface reflector combined with front texture will result in multiple scattering of light within the absorbing material and thereby increase the optical path length of light by multiple reflections. We intend to use TSSBR MPC as back surface passivation layer as well as back reflector for c-Si solar cells with Laser Fired Back contact. Other than photovoltaics there is a scope of possible application in microcavities and omnidirectional mirrors where the underlying principle remains the same.

Acknowledgement

This work was supported by the Ministry of New and Renewable Energy (MNRE) Govt. of India, through the project AMANSI under the National Solar Science fellowship program. We would like to thank NCPRE and CEN at IIT Bombay for the fabrication and characterization facilities and Grup d'Energia Solar of Universitat de Barcelona, Spain for the integration of MPC with the Silicon Solar cells. We would like to thank Amruta Joshi, Balraj Arunachalam and Thirumaliah N. for their help with different measurements.

References

Alcántara, S.P., Arangú, A.A.V., Plaza, G.S., 2014. The importance of optical characterization of PV backsheets in improving solar module power. In: 8th Int. Photovoltaic Power Generation Conf. Exhib.

Betancur, R., Romero-Gomez, P., Martinez-Otero, A., Elias, X., Maymó, M., Martorell, J., 2013. Transparent polymer solar cells employing a layered light-trapping architecture. Nat. Photonics 7, 995–1000. http://dx.doi.org/10.1038/nphoton.2013.276.

Biswas, R., Xu, C., 2012. Photonic and plasmonic crystal based enhancement of solar cells — Theory of overcoming the Lambertian limit. J. Non Cryst. Solids 358, 2289–2294. http://dx.doi.org/10.1016/j.jnoncrysol.2011.12.011.

Böscke, T.S., Kania, D., Helbig, A., Schöllhorn, C., Dupke, M., Sadler, P., Braun, M., Roth, T., Stichtenoth, D., Wütherich, T., Jesswein, R., Fiedler, D., Carl, R., Lossen, J., Grohe, A., Krokoszinski, H.-J., 2013. Bifacial n-type cells with > 20% front-side efficiency for industrial production. IEEE J. Photovoltaics 3, 674–677. http://dx.doi.org/10.1109/JPHOTOV.2012.2236145.

Chigrin, D.N., Lavrinenko, A.V., Yarotsky, D.A., Gaponenko, S.V., 1999. Observation of total omnidirectional reflection from a one-dimensional dielectric lattice. Appl. Phys. A Mater. Sci. Process. 68, 25–28. http://dx.doi.org/10.1007/s003390050849.

Colodrero, S., Forneli, A., López-López, C., Pellejà, L., Míguez, H., Palomares, E., 2012. Efficient transparent thin dye solar cells based on highly porous 1D photonic crystals. Adv. Funct. Mater. 22, 1303–1310. http://dx.doi.org/10.1002/adfm.201102159.

del Cañizo, C., del Coso, G., Sinke, W.C., 2009. Crystalline silicon solar module technology: Towards the 1 € per watt-peak goal. Prog. Photovoltaics Res. Appl. 17, 199–209. http://dx.doi.org/10.1002/pip.878.

Fischer, D., Dubail, S., Selvan, J.A.A., Vaucher, N.P., Platz, R., Hof, C., Kroll, U., Meier, J., Torres, P., Keppner, H., Wyrsch, N., Goetz, M., Shah, A., Ufert, K.-D., 1996. The "micromorph" solar cell: extending a-Si: H technology towards thin film crystalline silicon. In: Conference Record of the Twenty Fifth IEEE Photovoltaic Specialists Conference - 1996. IEEE, pp. 1053–1056. doi: http://dx.doi.org/10.1109/PVSC.1996.564311.

Florescu, M., Lee, H., Puscasu, I., Pralle, M., Florescu, L., Ting, D.Z., Dowling, J.P., 2007. Improving solar cell efficiency using photonic band-gap materials. Sol. Energy Mater. Sol. Cells 91, 1599–1610. http://dx.doi.org/10.1016/j.solmat.2007.05.001.

Goodrich, A., Hacke, P., Wang, Q., Sopori, B., Margolis, R., James, T.L., Woodhouse, M., 2013. A wafer-based monocrystalline silicon photovoltaics road map: Utilizing known technology improvement opportunities for further reductions in manufacturing costs. Sol. Energy Mater. Sol. Cells 114, 110–135. http://dx.doi.org/10.1016/J.SOLMAT.2013.01.030.

Haug, F.-J., Söderström, T., Cubero, O., Terrazzoni-Daudrix, V., Ballif, C., 2008. Plasmonic absorption in textured silver back reflectors of thin film solar cells. J. Appl. Phys. 104, 64509. http://dx.doi.org/10.1063/1.2981194.

Heiniger, L.-P., O'Brien, P.G., Soheilnia, N., Yang, Y., Kherani, N.P., Grätzel, M., Ozin, G.A., Tétreault, N., 2013. See-through dye-sensitized solar cells: photonic reflectors for tandem and building integrated photovoltaics. Adv. Mater. 25, 5734–5741. http://dx.doi.org/10.1002/adma.201302113.

Ingenito, A., Isabella, O., Solntsev, S., Zeman, M., 2014a. Accurate opto-electrical modeling of multi-crystalline silicon wafer-based solar cells. Sol. Energy Mater. Sol. Cells 123, 17–29. http://dx.doi.org/10.1016/J.SOLMAT.2013.12.019.

Ingenito, A., Isabella, O., Zeman, M., 2014b. Experimental demonstration of 4 n^2 classical absorption limit in nanotextured ultrathin solar cells with dielectric omnidirectional back reflector. ACS Photonics 1, 270–278. http://dx.doi.org/10.1021/ph4001586.

Ingenito, A., Luxembourg, S.L., Spinelli, P., Liu, J., Ortiz Lizcano, J.C., Weeber, A.W., Isabella, O., Zeman, M., 2016. Optimized metal-free back reflectors for high-efficiency open rear c-Si solar cells. IEEE J. Photovoltaics 6, 34–40. http://dx.doi.org/10.1109/JPHOTOV.2015.2487827.

Isabella, O., Dobrovolskiy, S., Kroon, G., Zeman, M., 2012. Design and application of dielectric distributed Bragg back reflector in thin-film silicon solar cells. J. Non Cryst. Solids 358, 2295–2298. http://dx.doi.org/10.1016/j.jnoncrysol.2011.11.025.

Ivanov, I.I., Nychyporuk, T.V., Skryshevsky, V.A., Lemiti, M., 2009. Thin silicon solar cells with SiO x / SiN x Bragg mirror rear surface reflector. Semicon. Phys. Quantum Electron. Optoelectron. 12 (4), 406–411.

Johnson, D.C., Ballard, I., Barnham, K.W.J., Bishnell, D.B., Connolly, J.P., Lynch, M.C., Tibbits, T.N.D., Ekins-Daukes, N.J., Mazzer, M., Airey, R., Hill, G., Roberts, J.S., 2005. Advances in Bragg stack quantum well solar cells. Sol. Energy Mater. Sol. Cells 87, 169–179. http://dx.doi.org/10.1016/j.solmat.2004.09.014.

Kim, S., Chung, J.-W., Lee, H.H.-M., Park, J., Heo, Y., Lee, H.H.-M., 2013. Remarkable progress in thin-film silicon solar cells using high-efficiency triple-junction technology. Sol. Energy Mater. Sol. Cells 119, 26–35. http://dx.doi.org/10.1016/j.solmat.2013.04.016.

Krc, J., Zeman, M., Luxembourg, S.L., Topic, M., 2009. Modulated photonic-crystal structures as broadband back reflectors in thin-film solar cells. Appl. Phys. Lett. 94, 153501–1535013. http://dx.doi.org/10.1063/1.3109781.

Kuo, M.Y., Hsing, J.Y., Chiu, T.T., Li, C.N., Kuo, W.T., Lay, T.S., Shih, M.H., 2012. Quantum efficiency enhancement in selectively transparent silicon thin film solar cells by distributed Bragg reflectors. Opt. Express 20, A828–A835.

Lunt, R.R., Bulovic, V., 2011. Transparent, near-infrared organic photovoltaic solar cells for window and energy-scavenging applications. Appl. Phys. Lett. 98, 113305. http://dx.doi.org/10.1063/1.3567516.

Manley, P., Yin, G., Schmid, M., 2014. A method for calculating the complex refractive index of inhomogeneous thin films. J. Phys. D. Appl. Phys. 47, 205301. http://dx.doi.org/10.1088/0022-3727/47/20/205301.

Mutitu, J.G., Shi, S., Barnett, A., Prather, D.W., 2010. Hybrid dielectric-metallic back reflector for amorphous silicon solar cells. Energies 3, 1914–1933. http://dx.doi.org/10.3390/en3121914.

O'Brien, P.G., Kherani, N.P., Chutinan, A., Ozin, G.A., John, S., Zukotynski, S., 2008. Silicon photovoltaics using conducting photonic crystal back-reflectors. Adv. Mater. 20, 1577–1582. http://dx.doi.org/10.1002/adma.200702219.

Raval, M.C., Joshi, A.P., Saseendran, S.S., Suckow, S., Saravanan, S., Solanki, C.S., Kottantharayil, A., 2015. Study of nickel silicide formation and associated fill-factor loss analysis for silicon solar cells with plated Ni-Cu based metallization. IEEE J. Photovoltaics 5, 1554–1562. http://dx.doi.org/10.1109/JPHOTOV.2015.2463741.

Soman, A., Antony, A., 2017. Broad range refractive index engineering of Si x N y and SiO x N y thin films and exploring their potential applications in crystalline silicon solar cells. Mater. Chem. Phys. 197, 181–191. http://dx.doi.org/10.1016/j.matchemphys.2017.05.035.

Soman, A., Antony, A., 2014. One-dimensional photonic crystal reflector using silicon-rich silicon nitride and silicon oxynitride multilayers for solar cells. In: 2014 IEEE 2nd International Conference on Emerging Electronics (ICEE). IEEE, pp. 1–4. doi: http://dx.doi.org/10.1109/ICEmElec.%202014.7151217.

Springer, J., Poruba, A., Müllerova, L., Vanecek, M., Kluth, O., Rech, B., 2004. Absorption loss at nanorough silver back reflector of thin-film silicon solar cells. J. Appl. Phys. 95, 1427. http://dx.doi.org/10.1063/1.1633652.

Tiedje, T., Yablonovitch, E., Cody, G.D., Brooks, B.G., 1984. Limiting efficiency of silicon solar cells. IEEE Trans. Electron Devices 31, 711–716. http://dx.doi.org/10.1109/T-ED.1984.21594.

Tobin, S.P., Vernon, S.M., Sanfacon, M.M., Mastrovito, A., 1991. Enhanced light absorption in GaAs solar cells with internal Bragg reflectors. In: The Conference Record of the Twenty-Second IEEE Photovoltaic Specialists Conference - 1991. IEEE, pp. 147–152, doi: http://dx.doi.org/10.1109/PVSC.1991.169199.

Tsai, Y.-L., Lin, C.-C., Han, H.-V., Chang, C.-K., Chen, H.-C., Chen, K.-J., Lai, W.-C., Sheu, J.-K., Lai, F.-I., Yu, P., Kuo, H.-C., 2013. Improving efficiency of InGaN/GaN multiple quantum well solar cells using CdS quantum dots and distributed Bragg reflectors. Sol. Energy Mater. Sol. Cells 117, 531–536. http://dx.doi.org/10.1016/j.solmat.2013.07.004.

Xifré Pérez, E., Design, fabrication and characterization of porous silicon multilayer optical devices, Ph.D. Thesis, Universitat Rovira i Virgili, Tarragona, 2007.

Xu, M., Bearda, T., Filipič, M., Sivaramakrishnan Radhakrishnan, H., Debucquoy, M., Gordon, I., Szlufcik, J., Poortmans, J., 2017. Damage-free laser ablation for emitter patterning of silicon heterojunction interdigitated back-contact solar cells. In: IEEE Photovoltaic Specialists Conference. doi: http://dx.doi.org/10.5281/ZENODO.844610.

Yablonovitch, E., 1987. Inhibited spontaneous emission in solid-state physics and electronics. Phys. Rev. Lett. 58, 2059–2062. http://dx.doi.org/10.1103/PhysRevLett. 58.2059.

Yablonovitch, E., 1982. Statistical ray optics. J. Opt. Soc. Am. 72, 899. http://dx.doi.org/10.1364/JOSA.72.000899.

Yablonovitch, E., Cody, G.D., 1982. Intensity enhancement in textured optical sheets for solar cells. IEEE Trans. Electron Devices 29, 300–305. http://dx.doi.org/10.1109/T-ED.1982.20700.

Yan, B., Yue, G., Owens, J., Yang, J., Guha, S., 2006. Over 15% efficient hydrogenated amorphous silicon based triple-junction solar cells incorporating nanocrystalline silicon. In: 2006 IEEE 4th World Conference on Photovoltaic Energy Conference. IEEE, pp. 1477–1480. doi: http://dx.doi.org/10.1109/WCPEC.2006.279748.

Yu, W., Shen, L., Shen, P., Meng, F., Long, Y., Wang, Y., Lv, T., Ruan, S., Chen, G., 2013. Simultaneous improvement in efficiency and transmittance of low bandgap semi-transparent polymer solar cells with one-dimensional photonic crystals. Sol. Energy Mater. Sol. Cells 117, 198–202. http://dx.doi.org/10.1016/j.solmat.2013.06.002.

Zeng, L., Bermel, P., Yi, Y., Alamariu, B.A., Broderick, K.A., Liu, J., Hong, C., Duan, X., Joannopoulos, J., Kimerling, L.C., 2008. Demonstration of enhanced absorption in thin film Si solar cells with textured photonic crystal back reflector. Appl. Phys. Lett. 93, 221105. http://dx.doi.org/10.1063/1.3039787.

Zeng, L., Yi, Y., Hong, C., Liu, J., Feng, N., Duan, X., Kimerling, L.C., Alamariu, B.A., 2006. Efficiency enhancement in Si solar cells by textured photonic crystal back reflector. Appl. Phys. Lett. 89, 111111. http://dx.doi.org/10.1063/1.2349845.

Zhou, D., Biswas, R., 2008. Photonic crystal enhanced light-trapping in thin film solar cells. J. Appl. Phys. 103, 93102. http://dx.doi.org/10.1063/1.2908212.